2-1-2011

Evidence for the Generation of Coherent Longitudinal Acoustic Phonons through the Resonant Absorption of Pulsed Far-Infrared Laser Radiation in Silicon Doping Superlattices

Thomas E. Wilson
Marshall University, wilsont@marshall.edu

Recommended Citation
Wilson TE. (2011) Evidence for the generation of coherent longitudinal acoustic phonons through the resonant absorption of pulsed far-infrared laser radiation in silicon doping superlattices. Chin. J. Phys. 49(1):118-126.

Evidence for the Generation of Coherent Longitudinal Acoustic Phonons through the Resonant Absorption of Pulsed Far-Infrared Laser Radiation in Silicon Doping Superlattices

Thomas E. Wilson[1,*]

[1] *Department of Physics, Marshall University, Huntington, USA*

(Received April 12, 2010)

We report the first experimental evidence for the direct excitation of coherent high-frequency acoustic phonons in semiconducting doping superstructures by electromagnetic fields of the same frequency. Nanosecond pulses of acoustic phonons have been detected by a superconducting bolometer at the appropriate time-of-flight across a (100) silicon substrate for ballistic longitudinal phonons when a silicon doping superlattice is illuminated with grating-coupled nanosecond-pulsed 246-GHz laser radiation with power density of $\sim$1 kW/mm^2. The absorbed phonon power density in the microbolometer is estimated to be $\sim$10 μW/mm^2, in agreement with theory. The phonon pulse duration matches the laser pulse duration. The absence of any detected transverse acoustic phonon signal by the superconducting bolometer is particularly striking. We believe these observations provide the first evidence that coherent zone-folded longitudinal acoustic phonons can be generated in a silicon doping superlattice and with negligible associated heat pulse generation, through the resonant absorption of grating-coupled pulsed far-infrared laser radiation.

PACS numbers: 63.20-e, 43.35.Gk, 68.65-Cd

I. INTRODUCTION

Coherent phonons in a variety of materials, including metal films, bulk semiconductors, and semiconductor heterostructures, have been studied for some time now, and different methods have been used for their generation and detection, including the ultrafast pump-probe techniques, as described in this and earlier conference proceedings - PHONONS 2007 [1]. Here, we investigate a different approach for coherent phonon generation, namely, that of the direct electromagnetic generation of coherent high-frequency monochromatic acoustic phonons in silicon doping superlattices (DSL) by high-peak-power, cavity-dumped far-infrared (FIR) laser radiation. Longitudinal acoustic waves are produced by exciting the superlattice with an electric field polarized *normal* to the alternately charged planes, and this field results from an evanescent surface wave generated by laser excitation of a grating coupler. This approach has the potential to produce intense pulses of high-frequency, narrow-bandwidth coherent acoustic phonons that have the desired polarization, with reasonable conversion efficiency and without the undesired concomitant broadband acoustic and/or optical phonon generation.

II. THEORY

A number of authors [2–5] have studied the effects, on the lattice dynamical properties of an otherwise homogeneous semiconductor, stemming from impurity charges associated with a microstructured one-dimensional periodic n and p-doping sequence, a so-called *nipi* doping superlattice. The phonon dispersion relation is nearly unchanged, as one might expect from a relative concentration of 10^{-3} impurity atoms or even less. The periodic space charge resulting from the doping superstructure, however, results in a unique prediction: longitudinal (LA) or transverse (TA) acoustic phonons, with wavevectors corresponding to odd multiples of the smallest reciprocal superlattice vector, may be directly excited by electromagnetic fields of the corresponding frequency with reasonable conversion efficiency. The frequency of the generated phonons is simply given by f = s/d**,** where$s$and $d$are the phase velocity for LA phonons and the superlattice period, respectively.

LA or TA phonons couple to electric fields normal or parallel to the DSL layers, respectively. The conversion efficiency ξ is defined as the ratio of the generated acoustic energy to the energy of the incident electromagnetic wave and is given by equation (1) (cgs units) below, where a is the host lattice constant (a simple cubic lattice is assumed), $n_D^{(2)}$ is the two-dimensional doping concentration, κ_0 is the dielectric constant, $M$is the atomic mass, $d$is the superlattice period, $c$is the speed of light, s is the longitudinal phonon velocity, $N$is the number of superlattice periods, and $r \equiv (d/a)$is the enlarged unit cell:

$$\xi \cong \left[\frac{\left(4\pi e^2 a^2 (n_D^{(2)})^2 (adN^2\right)}{(\kappa_0 M dr)(cs\sqrt{\kappa_0})} \right] \tag{1}$$

The upper limit to the two-dimensional (donor or acceptor) doping concentration is determined by the condition that there must be an effective bandgap. The limiting doping concentration follows from equations (1) and (8) in Dohler [2], and it is given in equation (2) below:

$$n_D^{(2)} \cong \left[\frac{(2E_g \kappa_0)}{(\pi d e^2)} \right] \tag{2}$$

where $E_g$is the host bandgap. In its ground state, the sample thus consists of alternately positively and negatively charged sheets of ions. Care must be taken to ensure that the sample has a closely balanced dopant concentration.

We have fabricated a small-period metallic grating coupler [6] on top of the DSL. Undesirable bulk broadband phonon generation might be expected in the absence of such a grating-coupling scheme, as a result of both multi-phonon and defect-induced absorption in the substrate. The grating coupler also serves to protect the sensitive superconducting bolometer detector from direct exposure to the intense FIR laser radiation, i.e., heat pulse generation in bolometers exposed to intense FIR laser pulses has been observed previously. The grating coupler is based on light diffraction on a periodically modulated surface. The grating coupler converts normally incident plane wave radiation into an evanescent surface

wave with a large electric field component *normal* to the charged planes for efficient LA phonon generation. Specifically, when the grating period becomes sufficiently small compared to the wavelength of the incident electromagnetic wave, the diffraction angle of the first-order wave in the substrate becomes imaginary and a diffracted (evanescent) surface wave is formed with a decay length δ given by equation (7) of [6]:

$$\delta \cong \left[\frac{p}{2\pi\sqrt{1-(np/\lambda)^2}} \right] \tag{3}$$

where p is the grating period and λ/n is the optical wavelength of the FIR in the DSL. The condition for the creation of an evanescent diffracted wave is given by $p/(\lambda/n)<1$. For a given δ, equation (3) may be inverted to find the optimum grating period p. We have used a grating period of $p \sim 10$ μm, resulting in a decay length of $\delta \sim 1.6$ μm, which is somewhat larger than the thickness of our DSLs. The larger p was chosen due to constraints imposed by our photolithography system. (n= 3.41 for silicon at 246 GHz). Niobium is used as the grating material because of its small surface resistance (i.e., low FIR absorption) below its superconducting transition temperature. We have used two different Nb film thicknesses, i.e., 100 nm and 500 nm.

III. EXPERIMENT

For our preliminary experiments reported upon herein, we have used a silicon delta-doped DSL consisting of 30 periods, fabricated upon a (100) float zone silicon substrate, with a period of length d= 34.5 nm,and with individual layers having a two-dimensional doping concentration $n_D^{(2)} = 8.5 \times 10^{12}$ cm^{-2}.The resulting conversion efficiency ξ for this DSL, using equation (1) above, is 9.6×10^{-9}.The period was chosen to match the LA phonon wavelength in silicon at a frequency (245.5 GHz) corresponding to a particularly strong FIR laser line (1.22 mm) produced by a $^{13}CH_3F$ gain medium. Future investigations would benefit by using DSL samples with a dramatically larger N.

We have previously developed [7] a cavity-dumped optically-pumped molecular-gas FIR laser resonator, and modified it for use at 1.22 mm as a source of intense ∼nanosecond pulses of p-polarized FIR laser radiation for these experiments. We cavity-dump the circulating resonator FIR radiation through the use of an optically switched intra-cavity intrinsic silicon wafer, oriented at the Brewster angle to the circulating p-polarized far-infrared radiation, through the absorption of above-bandgap radiation. The risetime of the cavity-dumped output pulse is on the order of a nanosecond, and the pulsewidth corresponds to the roundtrip time of the circulating FIR – 6 ns. Recent improvements to the FIR laser have included the following: (1) an in-situ mode-matching Newtonian telescope, employing custom TPX lenses, to couple the output into a 3-m long, 246-GHz corrugated waveguide for beam transport to the sample access window of the floor-mounted liquid helium cryostat, and (2) a recycling cryogenic absorption pump for the isotopic methyl fluoride gain medium. After the 246-GHz laser radiation propagates through our corrugated waveguide,

we routinely obtain power levels at the cryostat access window of 5 kW in 6-ns pulses, at a pulse repetition rate of 10 pulses per second. The DSL sample is installed at the end of an insertable sample rod, and the sample itself is contained in a split-cylinder metal-coated polymer jig that also holds a hyper-hemispherical silicon lens in contact with the grating coupler/DSL front sample surface. The jig also shields the bolometer from scattered FIR radiation. The focused FIR laser power density at the surface of the grating coupler/DSL is estimated to be $\sim$1 kW/mm^2 in a beamwaist of 3 mm.

The DSL sample assembly (rod and jig) is immersed in low-temperature liquid helium in a cryostat equipped with optical access. The temperature is established by pumping on the helium vapor through a precision computer-controlled butterfly valve with a vacuum pump. The temperature is typically held near 1.750 K (approximately 1/3 up the R-T curve for the superconducting bolometer detector) with a stability of 0.0002 K. Any resonantly excited phonons by pulsed FIR laser radiation are detected on the rear sample face (substrate thickness: 0.5 mm) by a superconducting granular aluminum bolometer/palladium bilayer microbolometer operating in a constant bias-current mode [8]. The active regions of our smaller bolometers are 100-nm thick, 10 micron $\times$ 20 micron granular aluminum capped with a 5-nm-thick palladium overlayer. (We will also use larger serpentine bolometers of the same material soon for increased phonon signal levels, but at this point, we have only used them to detect our attenuated FIR laser pulses.) We pattern both the Nb grating coupler and microbolometer using image-reversal optical lithography, dual-target dc-magnetron sputtering, and liftoff. When biased at 20 μA and 1.75 K, our smaller bolometers have a bare time constant (C/G) of 2.9 ns, and they have a calculated responsivity, R, at 50 MHz, of 9.8 kV/W. (The bandwidth associated with a 6-ns phonon pulse is 50 MHz.) Electrical contact is made to the bolometer with an MMCX microminiature coaxial jack that is integrated into the rear half of the split-cylinder sample jig. A 1-GHz bias tee passes the battery-powered dc-bias current through to the bolometer while allowing the ac-coupled bolometer output to be passed to a 1-GHz preamplifier (the latter has a voltage gain of 54). It was necessary to enclose the cryostat and bolometer electronics in a copper Faraday cage in order to shield the experiment from intense electromagnetic noise generated by the pulsed TEA CO_2pump laser and the pulsed frequency-doubled YAG laser (the latter induces the cavity-dumping of the FIR laser resonator).

Figure 1 below shows the response of the bolometer. We first observe (beginning near -225 ns) pulsed FIR laser radiation leaking through the 500-nm-thick superconducting niobium grating coupler (skin depth $\sim$ 39 nm). Next, we observe the onset of the large cavity-dumped FIR pulse near 0 ns (the cavity-dumped pulse has saturated the bolometer; hence, the pulse is seen to be larger in time than 6 ns, which is the observed FIR pulsewidth in earlier experiments). Finally, we observe a delayed ($\sim$65 ns) smaller pulse corresponding to the arrival for ballistic LA phonons that have traversed the 0.58-mm-thick (100) Si substrate. Figure 2 displays the bolometer response in nanowatts and at a higher time resolution; there is no evidence of either transverse ballistic or diffusive acoustic phonons.

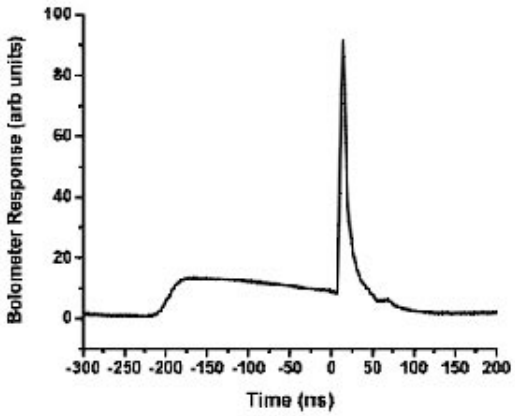

FIG. 1: Bolometer response (arbitrary units) 25 ns/div.

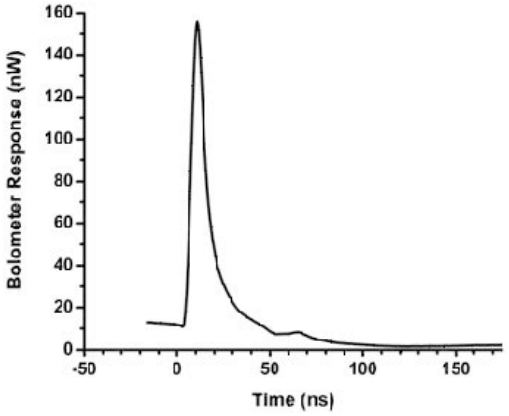

FIG. 2: Bolometer response (nW) 10 ns/div.

IV. DISCUSSION

A careful inspection of Figures 1 and 2 reveals the striking absence of any delayed ($\sim$98 ns) transverse acoustic phonon signal or diffusive phonon tail appearing in the bolometer response. The absence of this signature of incoherent phonons is to be compared to an earlier heat pulse experiment [8] on identical DSL samples; in that case, 0.5-μJ, 532-nm, 1-ns pulsed mini-YAG laser radiation was focused on the Nb grating coupler/DSL to a beam waist of 50 μm, and a similar (identical geometry and bias conditions) superconducting granular aluminum/Pd bolometer was used as the detector. The phonon signal from the heat pulse experiment is shown in Figure 3 below. In that heat pulse experiment, both LA and larger (due to phonon focusing) TA phonon signals were clearly observed at the appropriate delays relative to the initial pulse of scattered laser light reaching the bolometer. We take this to be evidence that there is very little incoherent heat pulse generation observed in our new results. It is also noteworthy that the absorbed power at the bolometer in the case of Figure 2 also matches closely the coherent power predicted by Ruden and Dohler [2] for our 200-μm^2 active area microbolometer, i.e., $\sim$2 nW.

V. CONCLUSIONS

We believe that we have strong evidence for the first experimental demonstration of the coherent generation of acoustic phonons in doping superlattices by pulsed FIR laser radiation. The phonon power, existing over an area of $\sim$1 mm^2 (focused FIR laser beamwaist), is estimated to be $\sim$10 μW. This power is in reasonable agreement with that predicted from the conversion efficiency noted above in equation (2), and our FIR laser pulse power,

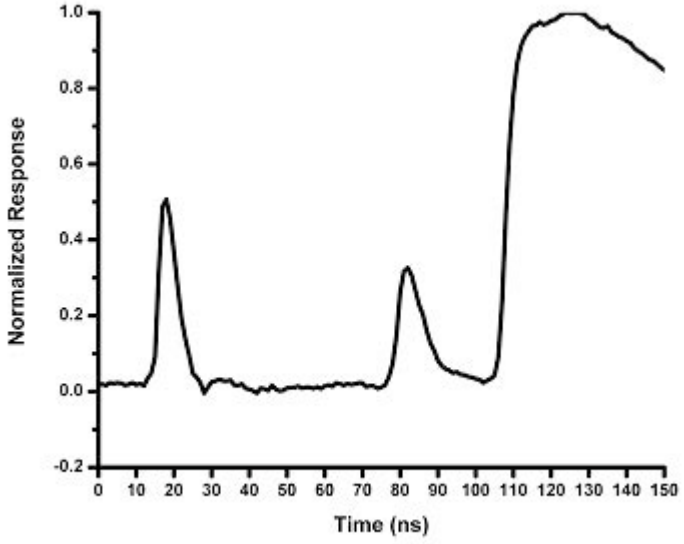

FIG. 3: Bolometer response for an earlier heat pulse experiment [8] conducted upon nearly identical DSL on (100) silicon samples with Nb grating couplers. The initial pulse near 10 ns is scattered laser light reaching the bolometer. The second pulse, appearing near 75 ns, corresponds to the appropriate time-of-flight (60 ns) for ballistic incoherent LA phonons across the 0.50-mm-thick (100) Si substrate. The last large signal commencing near 105 nm corresponds to the arrival of incoherent TA acoustic phonons, followed by a large diffusive tail.

i.e., from the theory of Ruden and Dohler [2]. The observed phonon pulse duration ($\sim$5 ns) in Figure 2 matches the FIR laser pulse duration. The absence of any detected transverse acoustic phonon signal by the superconducting bolometer is particularly striking. We believe these observations taken together provide strong evidence that coherent zone-folded longitudinal acoustic phonons can be generated in a silicon doping superlattice, and with negligible associated electronic or lattice heating, through the resonant absorption of grating-coupled pulsed far-infrared laser radiation. In the near future, we plan to increase the thickness of the Nb grating coupler to reduce the FIR laser radiation leakage detected by the bolometer, and to perform Si:B phonon spectroscopy on phonons generated by this process in new DSL samples with a significantly larger number of periods.

VI. FUTURE APPLICATIONS

One application of the novel coherent acoustic phonon source may be to extend the operating frequency of cryogenic acoustic microscopy into the sub-THz regime with a corresponding lateral resolution approaching the ultimate limit of $\sim$1 nm. The best cryogenic acoustic microscopes to date, operating at microwave frequencies, have had a maximum

resolution in the range of 20 nm and used sound waves produced from piezoelectric transducers in pressurized superfluid helium at 0.4 K [9]. In this frequency regime (15 GHz), three-phonon decay processes were shown to result in a depletion of the focused beam and to severely impact the signal to noise ratio [10]. However, above 209 GHz, it has been shown that both three- and four-phonon processes are negligible, and phonon mean free paths in superfluid helium, at temperatures up to 0.7 K, on the order of centimeters have been measured [11, 12]. In a pulse-echo mode, the superconducting granular aluminum bolometer can also be used as a sensitive detector whose time response matches that of the superlattice phonon generator. Due to the large impedance mismatch between solid samples and liquid helium, cryogenic reflection images contain information that is almost entirely topographic; however, as demonstrated by Foster [13], if the sample is "illuminated" from the rear with a simple heat pulse synchronized to the coherent signal pulse, there will be thermal phonons present near the beam focus; the scattering of the coherent phonons at the beam focus by these thermal phonons allows for the imaging of "shadowed" subsurface structures and defects. However, if the phonon source is sufficiently intense, enough transmission and reflection may occur to provide a sufficiently strong echo signal for subsurface imaging, even without the use of such "backlighting" as employed by Foster.

Granular aluminum bolometers can also function at sub-Kelvin temperatures with the application of a magnetic field parallel to the film [14]. In order to use bolometric detection of the phonon echo, we would fabricate a phonon "beamsplitter." A superlattice source/beamsplitter/bolometer detector cube of single-crystal silicon could be fabricated using direct wafer bonding. Twisted wafer bonding [15] creates bonds between two crystals that are essentially free of phonon-scattering defects, thereby exhibiting nearly perfect elastic transmission for high-frequency (∼300-GHz) phonons. Prior to direct-bonding, all crystal faces would undergo magneto-rheological finishing (MRF) [16], to minimize both surface roughness and sub-surface damage to prevent diffusive phonon scattering.

After the completion of successful pulse-echo experiments within the crystalline substrate, the next step would be to successfully transmit a coherent phonon beam into cold liquid helium using a phonon anti-reflection multilayer on the rear surface of the phonon beamsplitter cube. A phonon anti-reflection multilayer on the rear MRF-finished sample face for LA phonons could be fabricated using an amorphous ($a-$)silicon dioxide/silicon superlattice (ASL); the ASL as a high-frequency phonon filter has been reported by Koblinger *et al* [17]. For phonons propagating along a crystal symmetry direction and arriving at normal incidence upon a flat ASL, the anisotropy of the elastic constants may be ignored. Using the reported acoustic impedances [18] for the ASL and cold liquid helium [19], a simple characteristic matrix method calculation [20, 21] predicts a phonon transmissivity of greater than 99% for a multilayer stack consisting of 32 alternating quarter-wave layers of a:Si$0_2$and a:Si of thicknesses 5.0 and 8.6 nm, respectively. Santos *et al.* [22] have reported that phonons with a frequency as high as 600 GHz can easily traverse a large number (>200) of layers and interfaces of amorphous in a similar amorphous superlattice (Si:H and Si:N_x) without noticeable degradation. This implies that the coherence length of the phonons far exceeded the superlattice thickness (∼1 μm) of Santos. Since the ASL reported by Koblinger *et al.* has sharper filter characteristics than similar superlattices

formed of amorphous Si:H and Si:N_x, one may conclude that the thickness of an amorphous Si/$Si0_2$superlattice consisting of 32 layers should be much less than the coherence length of 246-GHz LA phonons. After coherent transmission into cold liquid helium, the propagating phonon pulse would arrive normally incident upon a MRF silicon surface at normal incidence and undergo specular reflection [23]. The echo would be subsequently detected by time-of-flight. A commercially available three-axis piezomotor-driven positioner specifically designed for use in low-temperature applications [24]would drive this silicon phonon mirror.

The final component to demonstrate the feasibility of a terahertz cryogenic acoustic microscope would be to fabricate a high-quality acoustic microlens on the rear silicon substrate and to apply the phonon anti-reflection multilayer, as described above, in order to focus the phonon beam onto a nanometer waist in HeII. Acoustic lenses suitable for operation at a lower frequency of 1 GHz have been fabricated by an isotropic chemical etch [25]. However, at terahertz frequencies, advanced dry etching techniques could be used to fabricate the precision acoustic microlens. Gray scale lithography and deep reactive ion etching might be used to fabricate a millimeter-diameter hemispherical acoustic lens with ∼mm focal lengths, with a spherical error under 15 nm rms and a surface roughness of approximately 2–8 nm (much less than phonon wavelengths).

Acknowledgments

We are thankful to Drs. Michael Oehme and Erich Kasper of the University of Stuttgart IHT, and to Dr. Hans-Joachim Gossmann for providing our delta-doped silicon doping superlattice samples. We also acknowledge the support of the United States NSF ECCS grant 0622060, and earlier, by support from the U.S. Army Research Office DAAD19-01-1-0466.

References

* Electronic address: wilsont@marshall.edu

[1] See Journal of Physics: Conference Series **92**, 012010-012032 (2007).
[2] P. Ruden and G.H. Dohler, Solid State Commun. **45** (1), 23 (1983).
[3] J.J. Quinn, U. Strom, and L.L. Chang, Solid State Commun. **45**, 111(1983).
[4] K. Dransfeld, *Rayleigh-Wave Theory and Applications*, eds. E.A. Ash and E.G.S. Paige (Springer, Berlin, 1985), p. 10.
[5] T.E. Wilson, JOSA **B6**, 1058 (1989).
[6] W.J. Li, B.D. McCombe, J. Appl. Phys. **71** (2) 1038 (1992).
[7] T.E. Wilson, *U.S. Department of Energy Strategic Defense Initiative's New and Innovative Concepts Program Summary Report*, edited by R. LeChevalier, (TPI Publishing, Falls Church, VA, 1989), pp. 79-80.
[8] T.E. Wilson, Journal of Physics: Conference Series **92**, 012180 (2007).
[9] M.S. Muha, A.A. Moulthrop, and G.C. Kozlowski, *Appl. Phys. Lett.* **56** (11), 1019-1021 (1990).
[10] K. Karaki, T. Saito, K. Matsumoto, and Y. Okuda, *Appl. Phys. Lett.* **59**, 908 (1991).

[11] M A H Tucker and A F G Wyatt , *J. Phys.: Condensed Matter* **4**, 7745 (1992).
[12] C.D.H. Williams, A.A. Zakharenko, and A.F.G. Wyatt, *J. Low Temp. Phys.* **126** (2) 591 (2002).
[13] John Foster and Daniel Rugar, *IEEE Trans. Sonics and Ultrasonics* **SU-32** (2) 139 (1985).
[14] H.W. M. Salemink, H. van Kempen, and P. Wyder, *J. Phys. C: Solid St. Phys.* **13**, 5089 (1980).
[15] M.E. Msall, A. Klimashov, W. Dietsche, K. Friedland, *Physica B* **263-264**, 361 (1999).
[16] D. W. Kim, J.W. Lee, M.W. Cho and S.B. Choi, *J. Physics: Conference Series* **149**, 012061 (2009).
[17] 0. Koblinger, J. Mebert, S. Dittrich, S. Dottinger, and W. Eisenmenger, *Phys. Rev.* ***B*** **35**, 9372 (1987); V. Narayanamurti, H.L. Stormer, M.A. Chin, A.C. Gossard, and W. Wiegmann, *Phys. Rev. Lett.* **43**, 2012 (1979).
[18] M. Rothenfusser, W. Dietsche, and H. Kinder, *Phonon Scattering in Condensed Matter (Springer Series in Solid-State Sciences 51)*, ed: W. Eisenmenger, K. Lassmann, and S. Dottinger,. 419-421 (1984).
[19] Ruslan V. Vovk, Charles D.H. Williams, and Adrian F.G. Wyatt, *Phys. Rev. B* 69, 144524 (2004).
[20] Max Born and Emil Wolf, *Principles of Optics*, 6th edition, (Pergammon Press, New York 1980), p. 70.
[21] H. Kato, *Phys. Rev.* ***B*** 59, 11136 (1999).
[22] P.V. Santos, L. Ley, J. Mebert and 0. Koblinger, *Phys. Rev.* ***B*** 36, 4548 (1987).
[23] H. Kinder, K. Weiss, *J. Phys.: Conden. Matter* **5**, 2063 (1993).
[24] Model ANSxyz100, *Attocube Systems AG,* München, Germany.
[25] H. Hashimoto, S. Tanaka, and K. Sato, *Jap. J. Appl. Phys., Part 1, 32, 5B*, 2543 (1993).